The Optimized Mechanical Structure Design of the Exoskeleton's Lower Limb Knee Joint Based on Sitting Posture Knee Rehabilitation

Tianchang Liu*
College of Mechanical and Automotive Engineering, Ningbo University of Technology, Ningbo, China

Abstract. This study aims to develop an exoskeleton device optimized for seated knee joint rehabilitation, designed in a modular manner, and it is divided into four key components: motion sensors, motor-worm gear units, thigh/shank fixation modules, and connecting pins. SolidWorks is utilized to construct a 3D model for verifying structural rationality, integrating worm gear transmission dynamics analysis, kinematic simulation, structural strength testing, and multi-condition adaptability research. The device incorporates self-centering mechanical structures, adaptive admittance control, and elastic joint stabilization technology. Moreover, the adaptive admittance control algorithm can dynamically adjust output torque based on real-time sensor feedback. Results indicate that the exoskeleton can be assembled and disassembled within 5 minutes, achieving a 60% volume reduction after disassembly. With a motion range of $0°\sim120°$ matching human physiological trajectories and a $40:1$ transmission ratio meeting driving force requirements, it is adaptable to patients with heights ranging from $150\sim185$cm and at different rehabilitation stages, enabling precise flexion-extension training and safety protection.

1 Introduction

Sitting for long periods poses significant risks to people recovering from knee joint injuries. Traditional rehabilitation methods often focus on walking training or static stretching, which are not well-suited to the unique biomechanical demands of sitting. This scenario highlights the necessity of designing rehabilitation tools specifically for sitting positions [1, 2].

The powered knee exoskeleton has demonstrated targeted assistive potential in the field of rehabilitation, but most existing designs focus on mobility functions, rather than sitting movements [3]. The main limitation of these devices when in a stationary state lies in the issue of joint alignment. If the exoskeleton lacks an adaptive alignment mechanism, parasitic forces and torques will be generated [3]. Studies have shown that the self-aligning mechanism (SAM) can reduce such parasitic forces by up to 97%[3].

*Corresponding author's email: Liu2794055162@outlook.com

The quality of human-machine physical interaction (pHRI) further influences the rehabilitation effect in sitting posture scenarios. Adaptive control strategies have been proven to enhance the performance of exoskeletons by considering the individual differences in driver dynamics and joint impedance [4]. Applying this principle to sitting posture scenarios with limited knee joint movement and requiring precise force control can optimize the assistance effect and achieve progressive joint movement.

Admittance control is the core technology of human-machine compliant interaction. Knee joint rehabilitation in the sitting position should be combined with ESP (Elastic Stability Protection) and PID control to ensure low-load interactive stability and avoid uncomfortable oscillations [1, 5, 6]. At the same time, the exoskeleton needs to be equipped with unified safety measures, automatically switching between "desired impedance mode" and "safe stop mode"[7].

This research has developed a specialized exoskeleton for knee joint rehabilitation in a sitting position. It integrates core technologies such as lightweight self-centering structure and adaptive impedance control, filling the gap in related rehabilitation needs and helping patients recover while promoting technological development.

2 Method

2.1 Design of exoskeleton framework and structural modeling

2.1.1 Overall framework design

This innovative sitting posture knee joint rehabilitation exoskeleton is composed of four independent and highly modular components - the motion sensor module, the motor-worm gear module, the thigh/calf fixation module, and the connecting pin. The modular architecture design is intended to meet three key requirements: simplifying maintenance (replaceable individual components), efficient space utilization (volume reduced by 60% after disassembly compared to assembled state), and adaptability to various rehabilitation scenarios (such as home, clinical or mobile treatment environments). Users can assemble or disassemble the system in 5 minutes without the need for special tools.

As shown in Fig. 1, the motion sensor module consists of a magnetic encoder, a torque sensor and an LED digital display. The magnetic encoder and the torque sensor are responsible for analyzing the joint movement status. After calculation, the rotation angle, rotation direction and rotation speed of the joint are displayed on the LED digital screen.

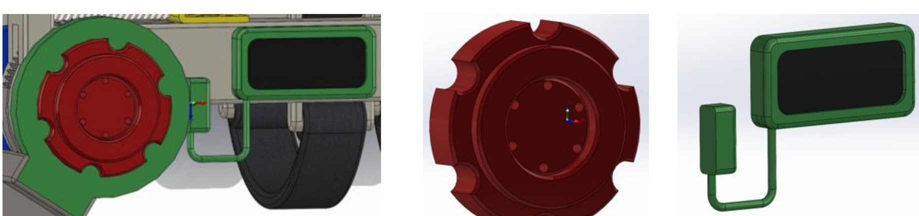

(a) Motion Sensor Module (b) Torque Sensor (c) Magnetic Encoder and LED Digital Display

Fig. 1. The motion sensor module consists of a magnetic encoder, a torque sensor and an LED digital display (Photo credit: Original)

As shown in Fig. 2, the motor-worm module consists of a motor, a worm, and a housing. The housing prevents foreign objects from entering during the operation of the worm, while the motor provides the power and the worm accomplishes the power transmission and reduction.

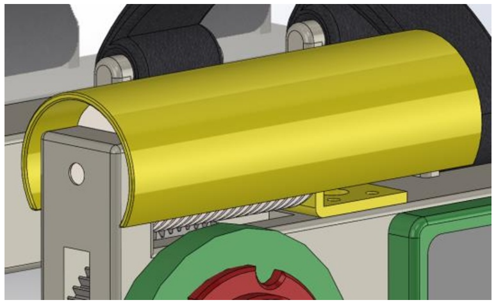

(a) Motor-Worm Gear Module and Enclosure

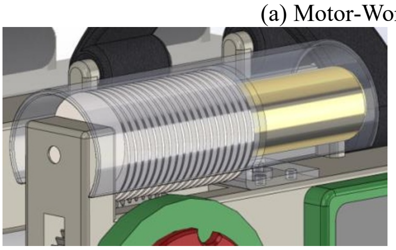

(b) Motors and Gears

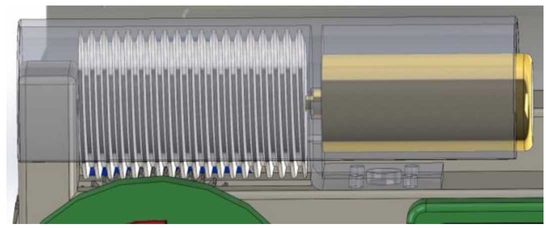

(c) Motors and Gears

Fig. 2. The motor-worm gear module is composed of a motor, a worm gear, and a housing (Photo credit: Original)

As shown in Fig. 3, the thigh/calf fixation module consists of elastic bands, length adjustment mechanisms and rigid support structures. The elastic bands and length adjustment mechanisms are used to fix the exoskeleton on the patient's limbs to accommodate patients of different body types, while the rigid support structures are used to stabilize the coordinated force of each module.

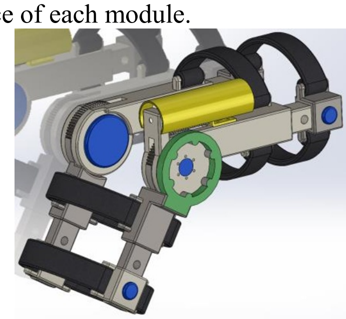

(a) Thigh/Calf Fixation Module

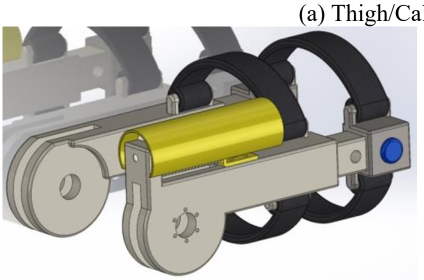

(b) Thigh Fixation Module

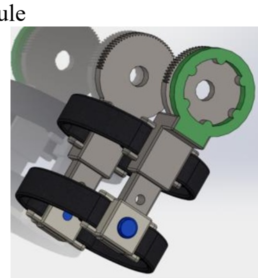

(c) Calf Fixation Module

Fig. 3. The thigh/calf fixation module consists of elastic bands, length adjustment mechanism and rigid support structure (Photo credit: Original)

As shown in Fig. 4, the large connecting pin connects the thigh/calf fixation module and serves as the rotating shaft for the upper gear of the calf fixation module. The small connecting pin fixes the length adjustment mechanism of the thigh/calf.

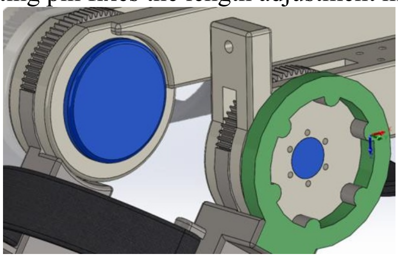

(a) Large-sized Connecting Pin for Connecting the Thigh/Calf Fixation Module

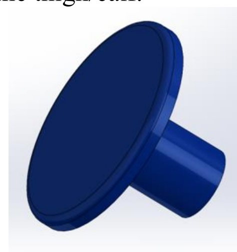

(b) Large Connecting Pin

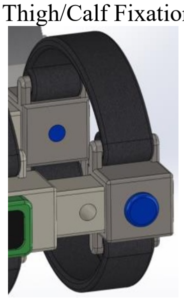

(c) Thigh Length Adjustment Mechanism

(d) Calf Length Adjustment Mechanism

Fig. 4. The large-sized connecting pin connects the thigh/leg fixation module, while the small-sized connecting pin fixes the length adjustment mechanism of the thigh/calf (Photo credit: Original)

2.1.2 Structural Modeling

The three-dimensional models of the key components of the exoskeleton were constructed using the computer-aided design (Solid Works) software, as shown in Fig. 5. In Fig. 5, the motion sensor module demonstrates the installation method and position of the module, as well as the collaborative relationship between the lower leg fixation module and the motion sensor module; the motor-worm gear module clearly presents the assembly relationship between the motor and the worm gear; the thigh/lower leg fixation module model shows the principle of the length adjustment mechanism and the design details of the straps; the connection pin module model not only reflects the connection function of the pin but also demonstrates its role as the rotating shaft of the upper end gear of the lower leg fixation module.

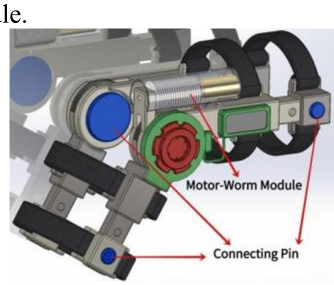

(a) Motor-Worm Gear Module and Connecting Pin

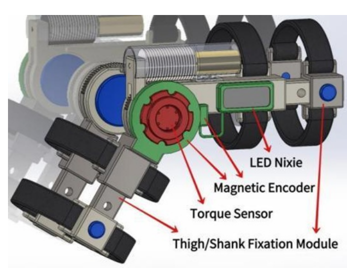

(b) Motion Sensor Module and Thigh/Calf Fixation Module

Fig. 5. Sitting posture knee joint rehabilitation exoskeleton—Solid Works modeling, which comprehensively verified the rationality of the structural design scheme (Photo credit: Original)

These models play a crucial verification role in the whole design process, whose core function is to examine the rationality of structural design schemes.

2.2 Theoretical analysis

2.2.1 Kinematic analysis of worm gear transmission

The worm gear transmission is the core transmission component of this exoskeleton.

The formula for calculating the transmission ratio i is

$$i = \frac{Z_2}{Z_1}$$

Here, Z_1 represents the number of teeth on the worm, and Z_2 represents the number of teeth on the worm wheel. In this design, $Z_1 = 1$ and $Z_2 = 40$, thus the transmission ratio $i = 40$. This high transmission ratio enables the motor to convert high speed and low torque into low speed and high torque, ensuring that the knee joint can obtain sufficient driving force during flexion and extension.

The self-locking condition is given by $\lambda \leq \rho_v$, where λ is the helix angle of the worm and ρ_v is the equivalent friction angle. The helix angle λ is determined by the formula.

$$\lambda = \frac{\rho_z}{\pi d_1}$$

It is calculated that among them, ρ_v represents the pitch of the worm, and d_1 represents the diameter of the worm's pitch circle. In this design, by selecting the parameters of the worm, the pitch angle λ is made smaller than the equivalent friction angle ρ_v, thereby ensuring the self-locking performance of the transmission system. That is, the worm cannot drive the worm gear in reverse, which can effectively prevent secondary injuries caused by equipment failures.

The formula for calculating efficiency η is

$$\eta = \frac{tan\lambda}{tan(\lambda + \rho_v)} \times 100\%$$

Although the worm gear transmission is less efficient compared to other transmission methods, considering its self-locking property and high transmission ratio, it remains the most suitable transmission method for this application scenario.

2.2.2 Structural strength analysis

The key components of the exoskeleton, such as the knee joint support and the worm gear, need to be ensured to be able to withstand the loads during the rehabilitation training process. The knee joint support bears bending and twisting loads during the movement of the knee joint. The material of the support is selected as aluminum alloy, which has the advantages of low density and high strength. The maximum stress of the support is less than the yield strength of the aluminum alloy, and using aluminum alloy material can ensure the safety of the structure. The worm gear bears compressive stress and shear stress during the power transmission process. The material of the worm gear is selected as 45# steel, which is treated by quenching and tempering to improve its strength and wear resistance. It can meet the strength requirements under the designed load.

2.3 Kinematics/control analysis

2.3.1 Kinematic analysis

The kinematic analysis of the exoskeleton knee joint was conducted to study the motion relationship among its various components during the knee joint flexion and extension process. The normal motion range of the human knee joint in seated rehabilitation training is 0°~120°. This exoskeleton was designed with a mechanical limit structure to control the motion range within this interval, in order to avoid secondary injuries caused by excessive flexion and extension. Therefore, the motion trajectory of the exoskeleton knee joint should match the anatomical motion trajectory of the human knee joint. Through kinematic analysis, it was verified that the motion trajectory of the designed exoskeleton knee joint is consistent with the natural motion trajectory of the human knee joint, ensuring the comfort and effectiveness of the rehabilitation training.

2.3.2 Control analysis

The control system of the exoskeleton is relatively simple. It mainly controls the forward and reverse rotation of the motors to achieve the flexion and extension of the knee joint. The main control strategy adopted is open-loop control, which controls the motor to rotate at a fixed speed and angle according to the preset program. Due to the self-locking performance of the transmission system, no complex closed-loop control is required, which simplifies the control system and reduces costs. At the same time, the motor needs to be selected based on the torque and speed requirements of the knee joint movement. The rated torque of the motor should be able to meet the maximum load during the knee joint movement, and its rated speed should match the transmission ratio of the worm gear transmission to ensure that the knee joint can obtain the appropriate movement speed.

2.4 Analysis of motion states under different operating conditions

Firstly, patients at different rehabilitation stages have different requirements for the range of motion and driving force of the knee joint. For patients in the early stage of rehabilitation, the range of motion is set at 0°~60°, and the driving force is relatively small. For patients in the later stage of rehabilitation, the range of motion can gradually be expanded to 0°~120°, and the driving force can also be appropriately increased. This exoskeleton is designed with adjustable limit structures for angles and adjustable motors for output torque to meet the needs of different rehabilitation stages. Secondly, patients of different body types have differences in the length of their lower limbs and the force exerted on the knee joint. The tightening and loosening adjustment structure of the lower leg and thigh fixation modules can be adapted to patients with heights ranging from 150~185cm. Through simulation verification, this exoskeleton can maintain the correct movement trajectory under different body types. Finally, the movement speed of the knee joint also affects the rehabilitation effect and user comfort. The exoskeleton can control the movement speed of the knee joint by adjusting the motor speed and controlling the motor to work within an appropriate speed range to ensure the best rehabilitation effect.

3 Results

3.1 Component modeling and assembly performance

The three-dimensional model of the key components of the exoskeleton constructed by Solid Works effectively verified the rationality of the structural design. As shown in Fig. 6, the motion sensing module (integrating magnetic encoder, torque sensor and LED digital display) achieved precise installation and stable cooperation with the lower leg fixation module. The assembly structure of the motor-worm gear module ensured the reliability of power transmission. The telescopic design of the thigh/lower leg fixation module and the "connection-rotary shaft" dual function of the connecting pin met the requirements of modular design. The spatial layout verification indicated that there was no functional interference among the components and the overall structure had no redundancy. The assembly simulation showed that the user could complete disassembly and assembly within 5 minutes without special tools, and the volume after disassembly was reduced by 60% compared to the assembled state, meeting the requirements for convenient storage and portability.

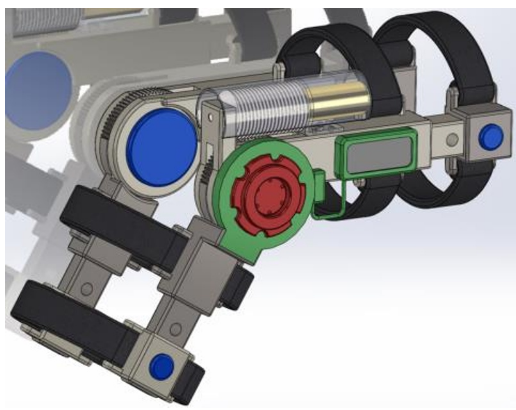

Fig. 6. The three-dimensional model of the key components of the exoskeleton, constructed using Solid Works effectively verified the rationality of the structural design (Photo credit: Original)

3.2 Kinematic simulation results

The kinematic analysis verified the motion performance of the exoskeleton within the designed range. As shown in Fig. 7, the robot model based on the modified Denavit-Hartenberg (DH) parameters includes thigh links (220cm) and calf links (170cm), and the knee joint motion range is constrained within 0°~120° by the mechanical limit structure. The posture simulation results show that at the initial posture (knee joint 0°), the thigh and calf are aligned horizontally; in the mid-range posture (flexion 60°), the joint bends smoothly; at the maximum flexion posture (120°), it fully conforms to the physiological movement trajectory of the human body. The trajectory planning simulation (200 steps) generated smooth joint position, velocity, and acceleration curves. The knee joint position trajectory linearly transitions from 0°~120°, while the ankle joint remains fixed at 0°, and there are no sudden changes in speed and acceleration. The end effector (ankle joint) presents a straight trajectory in the xy plane, confirming consistency with the anatomical movement characteristics of the human knee joint.

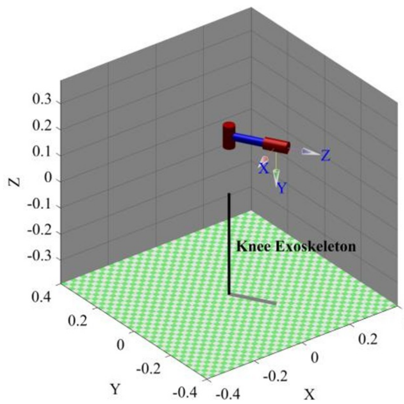

(a) The robot model established based on the modified DH parameters

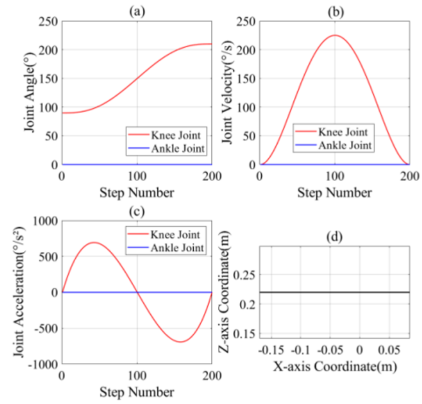

(b) Trajectories of Position, Velocity and Acceleration of the Knee and Ankle Joints, and the Linear Trajectory of the Ankle Joint

Fig. 7. Kinematic analysis verified the motion performance of the exoskeleton within the designed range, confirming its consistency with the anatomical motion characteristics of the human knee joint (Photo credit: Original)

3.3 Dynamic performance analysis

3.3.1 Gravity load simulation

Based on the gravity load analysis of the exoskeleton's dynamic parameters (thigh mass: 5.0kg, calf mass: 3.0kg), as shown in Fig. 8, three-dimensional surface graphs of joint torques under different joint angles were generated. The gravity torque of the knee joint increases as the flexion angle increases. When the knee joint angle changes from $0°\sim120°$, the torque range is approximately $77.6N\cdot m$ to $79.4N\cdot m$; the gravity torque of the ankle joint remains relatively stable within the $\pm30°$ range of ankle joint movement. This distribution indicates that the motor output torque matching the worm gear transmission with a $40{:}1$ ratio can completely counteract the gravity load during rehabilitation training.

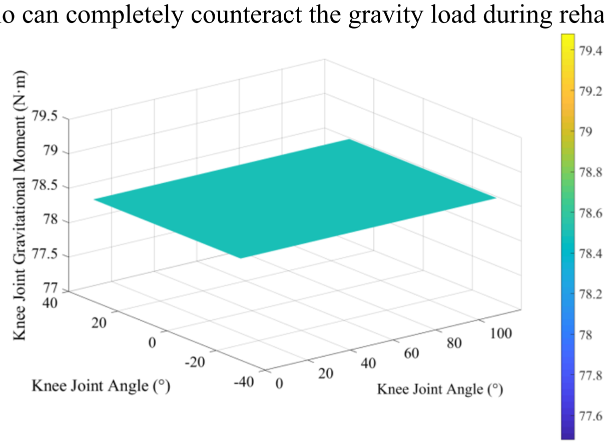

Fig. 8. The three-dimensional surface plots of joint torques at different joint angles show that the output torque of the motor can completely counteract the gravitational load during rehabilitation training (Photo credit: Original)

3.3.2 Inertial matrix and dynamic operating degree

The inertia matrix simulation reveals the dynamic characteristics of the exoskeleton links. As shown in Fig. 9, within the joint angle range of $-60°\sim60°$, elements M_{11}(hip inertia), M_{12}(coupling inertia), and M_{22}(calf inertia) all fall within the stable range. Specifically, $M_{11} \approx 0.4\sim0.9kg \cdot m^2$, $M_{12} \approx 0.1\sim0.9kg \cdot m^2$, and $M_{22} \approx 2.0\sim3.5kg \cdot m^2$, indicating good consistency in dynamic response. The dynamic operational degree analysis under the non-singular joint configuration $[0.3rad, 0.5rad]$ yielded a well-conditioned Jacobian matrix $J(6 \times 2)$ and inertia matrix $M(2 \times 2)$. By introducing a small perturbation ($\varepsilon = 1^{e-6}$) to avoid singularity calculation of the dynamic operational degree matrix M_x, a nearly spherical operational degree ellipsoid was generated, confirming uniform force transmission within the working space and good motion flexibility. The position dynamic operational degree index $[det({M_x}^{0.5})]$ indicates that the exoskeleton can achieve smooth and controllable motion in low-speed rehabilitation tasks.

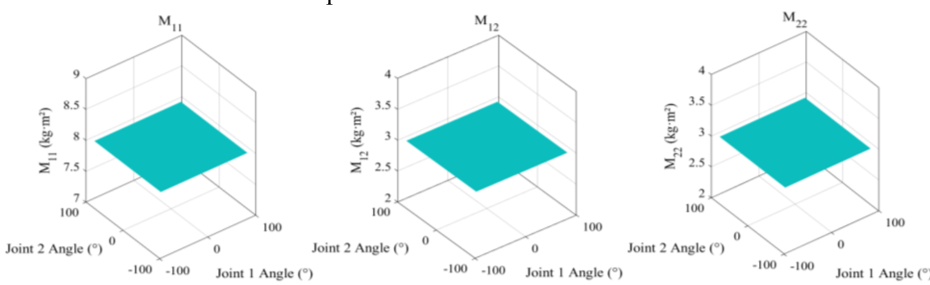

(a) Simulation of the Inertia Matrices for Elements M_{11}(Hip Inertia), M_{12}(Coupling Inertia), and M_{22}(Calf Inertia)

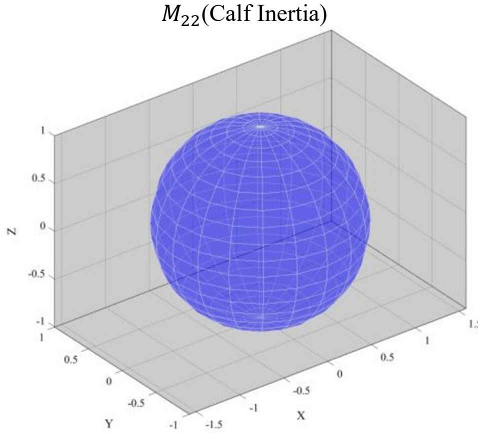

(b) Kinetic Operating Degree Matrix

Fig. 9. The simulation of the inertia matrix reveals the dynamic characteristics of the exoskeleton linkage, indicating that the dynamic response is highly consistent. The exoskeleton can achieve smooth and controllable movement in low-speed rehabilitation tasks. (Photo credit: Original)

3.3.3 Mechanical transmission and structural strength

The analysis and verification of worm gear transmission have confirmed the key performance indicators: a $40:1$ transmission ratio is highly efficient in converting the high-speed low-torque output of the motor into the low-speed high-torque drive required by the knee joint. Through parameter optimization, the self-locking condition $(\lambda \leq \rho_v)$ is met, which can prevent secondary damage caused by reverse drive.

3.4 Operational adaptability

The exoskeleton demonstrates strong adaptability to diverse user needs. For different rehabilitation stages, adjustable angle limits (0° ~60° in the early stage and 0° ~120° in the advanced stage) and variable motor torque can be adjusted to meet the requirements of progressive training. The adjustable straps of the thigh/calf fixation module are suitable for users with heights ranging from 150~185cm. Kinematic simulation has confirmed that the movement trajectories of users of different body types are consistent. Adjusting the motor speed can keep the knee joint movement within the optimal range, balancing the rehabilitation effect and user comfort without affecting stability.

3.5 Discussion

The improved adaptive admittance control optimally adapts to the static-dynamic mixed characteristics of the sitting-knee joint movement, which can further reduce the human output energy and high-frequency vibrations [8, 9]. Moreover, the combination of open-loop control and the self-locking ability of the worm gear transmission $(\lambda \leq \rho_v)$ can automatically respond to abnormal forces through a unified safety metric, avoiding unexpected injuries [10].

4 Conclusion

This research, in response to the unique requirements of knee joint rehabilitation in a seated position, successfully designed a modular and optimized exoskeleton device. This effectively filled the gap in the application of traditional rehabilitation tools in seated scenarios, providing precise and adaptable rehabilitation solutions for patients with knee joint injuries, stroke, and degenerative diseases.

The research achieved a breakthrough in the core technology through targeted design: By adopting a modular decomposition strategy, the device was divided into four components: motion sensor, motor-worm gear, thigh/calf fixation, and connecting pin. The structural rationality was verified through Solid Works 3D modeling. The disassembly and assembly could be completed within 5 minutes, and the volume was reduced by 60% after disassembly, achieving a balance between portability and maintenance convenience.

This exoskeleton demonstrates excellent adaptability to various working conditions. Through angle limit adjustment, adjustable torque, and length adaptation design, it can meet the individual needs of people with a height ranging from 150~185cm and patients at different rehabilitation stages. The training mode can be switched between 0° ~60° for early rehabilitation and 0° ~120° for advanced stages, achieving the goal of progressive rehabilitation.

In conclusion, this study develops a safe, comfortable sitting-knee rehabilitation exoskeleton, provides R&D references, and will optimize it to boost clinical application value.

References

1. M. Keppler, C. Raschel, D. Wandinger, A. Stemmer, and C. Ott, Robust stabilization of elastic joint robots by ESP and PID control: Theory and experiments. IEEE Robot.

Autom. Lett. 7(3), 8283–8290 (2022)

2. T. M. Kwok and H. Yu, Asymmetric bimanual ADL training with underactuated exoskeleton using independent joint control and visual guidance. IEEE Access **12**, 9277–9291 (2024)
3. S. V. Sarkisian, M. K. Ishmael, and T. Lenzi, Self-aligning mechanism improves comfort and performance with a powered knee exoskeleton. IEEE Trans. Neural Syst. Rehabil. Eng. 29, 629–640 (2021)
4. Z. Li, Q. Li, P. Huang, H. Xia, and G. Li, Human-in-the-loop adaptive control of a soft exo-suit with actuator dynamics and ankle impedance adaptation. IEEE Trans. Cybern. **53**(12), 7920–7932 (2023)
5. Z. Li, B. Huang, Z. Ye, M. Deng, and C. Yang, Physical human–robot interaction of a robotic exoskeleton by admittance control. IEEE Trans. Ind. Electron. **65**(12), 9614–9624 (2018)
6. T. Ma, S. Yin, Z. Hou, H. Yu, and C. Fu, Real-world terrain-dependent variable admittance model for amputee–prosthesis system and environment interaction. IEEE/ASME Trans. Mechatronics (2025)
7. A. Calanca, E. Dimo, E. Palazzi, and L. Luzi, Enhancing force controllability by mechanics in exoskeleton design. Mechatronics **86**, 102867 (2022)
8. N. Sun, G. Li, and L. Cheng, Design and validation of a self-aligning index finger exoskeleton for post-stroke rehabilitation. IEEE Trans. Neural Syst. Rehabil. Eng. **29**, 1513–1523 (2021)
9. J. Kou, Y. Wang, Y. Shi, S. Xu, H. Zhan, and Q. Guo, Active control strategy of lower limb exoskeleton based on variable admittance control. Robot. Auton. Syst. **186**, 104906 (2025)
10. X. Li, Y. H. Liu, and H. Yu, Adaptive impedance control for compliantly actuated robots with a unified safety measure. In Proc. World Congr. Intell. Control Autom. (WCICA), pp. 444–449 (2018)